Real-Time Nonlinear Model Predictive Control for Microgrid Operation

Armin Nurkanović, Amer Mešanović, Andrea Zanelli, Gianluca Frison, Jonathan Frey,
Sebastian Albrecht, Moritz Diehl

***Abstract*— We present a real-time feasible Nonlinear Model Predictive Control (NMPC) scheme to control a microgrid described by a detailed Differential Algebraic Equation (DAE). Our NMPC formulation allows to consider secondary voltage and frequency control, steady-state equal load sharing, economic goals and all relevant operational constraints in a single optimization problem. The challenge is to control the fast and large dynamical system in real-time. To achieve this goal, we use the recently introduced Advanced Step Real-Time Iteration (AS-RTI) scheme and its efficient implementation in the `acados` software package. We present an NMPC scheme which delivers feedback in the range of milliseconds. Thereby, the controller responds efficiently to large disturbances and mismatches in the predictions and effectively controls the fast transient dynamics of the microgrid. Our NMPC approach outperforms a state-of-the-art I-controller usually used in microgrid control and shows minor deviation to a fully converged NMPC approach.**

I. Introduction

Nonlinear Model Predictive Control (NMPC) is a practical and advanced control strategy which uses dynamical models to predict the system's future behavior and to establish an optimal control response. The performance of NMPC schemes relies on the accuracy of the used model and computational resources available. This control strategy enables one to incorporate nonlinear dynamic models, constraints, economic and operational goals into an Optimal Control Problem (OCP) in a natural way.

Microgrids (MGs) are small electrical power grids consisting usually of Distributed Energy Resources (DER), such as small distributed generators and Renewable Energy (RE) devices, storage devices and loads. They can be operated independently as a single controllable unit either in island mode or be connected to a large power system through a point of common coupling [1]. NMPC is a convenient strategy to control an MG as a whole and to ensure fulfillment of several different goals such as: a) satisfaction of frequency and voltage limits [2], b) coverage of time-varying demands [3], c) higher integration of RE devices and thus reduction of carbon emissions [1], d) fulfillment of economic goals such as reducing the fuel costs [1] and e) equal share of the load between controllable DERs [2]. Moreover, energy and fuel price, demand and RE production predictions can naturally be incorporated into the OCP and feedback accounts for mismatches in the predictions and uncertainties in model parameters.

State-of-the-art power system control is hierarchical, where each hierarchy operates in a different time-scale to avoid undesired interactions between hierarchies [4]. Primary control ensures power system stability and instantaneous power balance with distributed controllers. However, in general even when stabilization is successfully achieved, frequency and voltage deviate in steady state from their reference values, which leads to the next control level [4]. Secondary control (SC) ensures removal of the deviation while providing reference trajectories for the primary controllers. It is in the time-scale of up to several minutes and typically realized with a centralized I-controller. Tertiary control ensures that the power system operates in a cost-effective manner in larger time-scales by using steady-state models. This separation of time-scales is necessary in order to avoid cross-coupling between the control hierarchies and potential instability. In this work, we propose NMPC for the SC of MGs while considering short-term economic goals and load sharing. This shortens the time-scale of SC significantly, as the power system dynamics can be directly considered for the SC. In MG control, hierarchical control approaches are common [5] in order to reduce computational complexity [3], [6], to account for communication link limitations [7], [2] and to handle different time-scales [8]. To further reduce the computational load, distributed MPC approaches are common in MG and power systems control [2], [9], [3], [10].

Many Model Predictive Control (MPC) approaches for operation and control of MGs in the literature consider tertiary control, i.e. unit commitment and economic dispatch, see [8], [11], [3] and references therein. The goal is usually to minimize the overall operating cost and to meet the predicted load demand. In such cases the prediction horizon is usually in the range of 24 to 48 hours. The system is considered to be in steady state and, to further reduce the complexity, simplified linear models are used [1]. The time-step of the discrete time system is usually between 15 minutes and

This research was supported by the German Federal Ministry of Education and Research (BMBF) via the funded Kopernikus project SynErgie (03SFK3U0) and the AlgoRes project (01S18066B), by the German Federal Ministry for Economic Affairs and Energy (BMWi) via eco4wind (0324125B) and DyConPV (0324166B), and by DFG via Research Unit FOR 2401.

Armin Nurkanović is with Siemens Corporate Technology, 81739 Munich, Germany and the Department of Microsystems Engineering (IMTEK) University Freiburg, 79110 Freiburg, Germany Amer Mešanović and Sebastian Albrecht are with Siemens Corporate Technology, 81739 Munich, Germany {armin.nurkanovic,amer.mesanovic, sebastian.albrecht}@siemens.com

Andrea Zanelli, Gianluca Frison and Jonathan Frey are with the Department of Microsystems Engineering (IMTEK) and Moritz Diehl is with the Department of Microsystems Engineering (IMTEK) and Department of Mathematics, University Freiburg,79110 Freiburg, Germany {andrea.zanelli, gianluca.frison, jonathan.frey moritz.diehl}@imtek.uni-freiburg.de

one hour. In general, this results in a Mixed-Integer Linear Programing (MILP) formulation, whereas stability and SC is assumed to be handled by lower level controllers [8].

Several MPC based SC approaches consider multi-area interconnected power grids [10], [9]. In these systems, each subsystem is modeled with aggregate models to represent the behavior of local grids, which are connected with tie-lines. In [10] the MPC controller for SC outperforms state-of-the-art PI controllers in various scenarios. In these works, voltage control is usually not treated explicitly by the MPC controller, as large power transmission systems are considered, in which voltage and frequency control can be decoupled due to low resistances in the system. In MGs, however, the coupling of voltage and frequency is typically stronger due to different parameters of the power system [12], and approaches are needed which consider both. Hence, in islanded MGs, frequency and voltage need to be controlled at the same time. In [2], [7], [13] the authors propose an MPC approach for SC. However, [7] uses a simplified model for the grid frequency without additional constraints, and the resulting OCP is solved analytically. In [2], a distributed linear MPC approach is taken for SC of voltage and frequency. In [13] a real-time feasible NMPC scheme for voltage and frequency control of one diesel generator is reported.

A. Contributions and Outline

In this paper we present a centralized real-time feasible NMPC scheme for operation of an islanded MG modeled by a DAE of index 1. We consider a six-bus MG obtained with a modular modeling approach described in Section III. To the best of our knowledge, this is the first real-time feasible NMPC approach that combines economic goals, voltage and frequency control, and load sharing. Furthermore, we modeled the fast nonlinear dynamics in detail. To achieve real-time feasibility and decrease suboptimality we use the Advanced Step Real-Time Iteration (AS-RTI) for DAEs [14], [15] and an efficient implementation of it via `acados` [16].

Section II briefly introduces NMPC, the methods and software used in this paper. Afterwards, in Section III, the proposed modular modeling approach for MGs is outlined. In Section IV, we describe the goals of our NMPC scheme and all relevant constraints. Finally, in Section V, we present simulation experiments to compare our developed approach to a state-of-the-art I-controller and a fully converged NMPC controller, before we conclude this work with Section VI.

II. Nonlinear Model Predictive Control

In real-time NMPC one has to solve computationally expensive optimization problems online on hardware often with limited computational power. Depending on the application, the dynamics might be fast and modeled by large and complex DAEs, as in this paper. The challenge can be both in simulating and generating the sensitivities needed for the optimization algorithm. However, recent progress both in numerical methods [17], [14], [18] and software [16], [19] for NMPC enables one to use real-time feasible NMPC even for challenging industrial applications involving short sampling times.

A. Problem Formulation

The MG is be modeled by a continuous time semi-explicit DAE, of the form

$$\dot{x}(t) = f(x(t), u(t), z(t), p(t)), \tag{1a}$$
$$0 = g(x(t), u(t), z(t), p(t)), \tag{1b}$$

that is assumed to be of index 1, i.e. the Jacobian $\frac{\partial g(\cdot)}{\partial z}$ is invertible. Hereby, $x(t) \in \mathbb{R}^{n_x}$ are the differential states, $z(t) \in \mathbb{R}^{n_z}$ the algebraic variables, $u(t) \in \mathbb{R}^{n_u}$ the control inputs and $p(t) \in \mathbb{R}^{n_p}$ are time-varying parameters.

We will consider the following discrete time OCP structured NLP with DAEs, which one can obtain with the Direct Multiple Shooting parameterization [20] of a continuous time OCP:

$$\min_{\substack{u_0,\dots,u_{N-1}\\ z_0,\dots,z_{N-1}\\ x_0,..x_N}} \quad \sum_{i=0}^{N-1} l_i(x_i, z_i, u_i) + l_N(x_N) \tag{2a}$$
$$\text{s.t.} \quad x_0 - \hat{x}_0 = 0, \tag{2b}$$
$$x_{i+1} - \Phi(x_i, z_i, u_i, p_i) = 0,\ \forall i \in \mathcal{I}, \tag{2c}$$
$$g(x_i, z_i, u_i, p_i) = 0,\ \forall i \in \mathcal{I}, \tag{2d}$$
$$h(x_i, u_i, z_i) \geq 0, \forall i \in \mathcal{I}, \tag{2e}$$
$$r(x_N) \geq 0. \tag{2f}$$

Here, $N \in \mathbb{N}$ is the horizon length and $\mathcal{I} \coloneqq \{0, \dots, N-1\}$ is the index set. The optimization variables are $x_i \in \mathbb{R}^{n_x}$, $z_i \in \mathbb{R}^{n_z}$, $u_i \in \mathbb{R}^{n_u}$, $p_i \in \mathbb{R}^{n_p}$ are time varying parameters, the objective function contributions $l_i : \mathbb{R}^{n_x} \times \mathbb{R}^{n_z} \times \mathbb{R}^{n_u} \to \mathbb{R}$ and $l_N : \mathbb{R}^{n_x} \to \mathbb{R}$. The function $\Phi : \mathbb{R}^{n_x} \times \mathbb{R}^{n_z} \times \mathbb{R}^{n_u} \times \mathbb{R}^{n_p} \to \mathbb{R}^{n_x}$ denotes the state transition map, which is obtained by some numerical integration scheme for DAEs, and $g : \mathbb{R}^{n_x} \times \mathbb{R}^{n_z} \times \mathbb{R}^{n_u} \times \mathbb{R}^{n_p} \to \mathbb{R}^{n_z}$ collects the discretized algebraic equations of the model (1). The functions $h : \mathbb{R}^{n_x} \times \mathbb{R}^{n_z} \times \mathbb{R}^{n_u} \to \mathbb{R}^{n_h}$ and $r : \mathbb{R}^{n_x} \to \mathbb{R}^{n_r}$ define the inequality constraints and $\hat{x}_0$ denotes the initial state. We assume all functions to be at least two times continuously differentiable.

In an NMPC setting, an instance of the Nonlinear Program (NLP) (2) is being (approximately) solved online at every sampling instant. After the optimization problem is solved, the first part of the discrete control trajectory u_0 is passed to the process. As soon as a new state-estimate $\hat{x}_0$ is available, it is embedded in the corresponding instance of (2). For a clearer notation we will omit the time dependency for all variables.

B. Real-Time NMPC Algorithms and Software

To solve the NLP (2) online and meet the real-time requirements, often one cannot simply use an off-the-shelf optimization solver. For complex problems, the computational complexity will induce large feedback delays which can severely degrade the NMPC controller performance. Therefore, we use a tailored real-time feasible NMPC scheme

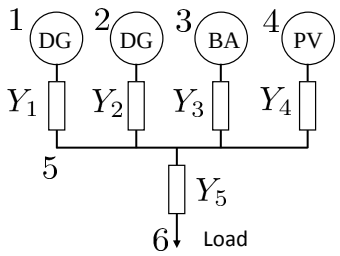

Fig. 1. Structure of the considered microgrid.

namely the AS-RTI, for details see [14], [15], which is an extension of the well known Real-Time Iteration (RTI) [21]. In the RTI scheme, a single Sequential Quadratic Programming (SQP) iteration is performed per sampling time. The computations are divided into a *preparation phase* and a *feedback phase*. Due to the linearity of (2b), in the preparation phase all derivative and function evaluations can be performed without the knowledge of the next state estimate $\hat{x}_0$. When a new state estimate is available, in the feedback phase just a single Quadratic Problem (QP) is solved, hence the feedback delay is reduced. In order to improve convergence, in the AS-RTI, in the preparation phase a few additional computations are performed on an *advanced problem*, i.e. an OCP with a predicted initial value $\tilde{x}_0$ at time when the next feedback is needed. Depending on the available time, the additional computations can range from solving a single additional QP up to several (inexact) SQP iterations, for details see [14], [15].

The AS-RTI can efficiently be implemented using the modular open-source software package `acados` [16] and its MATLAB interface. This package provides a collection of embedded optimization and simulation algorithms written in `C` which use the linear algebra library `BLASFEO` [22]. This library provides efficient routines tailored for different CPU architectures. An important ingredient for the reduction of the feedback delay is to solve intermediate QPs quickly. In this work, we use `HPIPM`, an interior-point based QP solver [19], within the SQP.

III. Microgrid Model

Figure 1 shows the schematic illustration of the MG considered in this work. Many practically relevant MGs share a similar structure [23]. Note that the system consists of heterogeneous, asymmetrically connected components. It consists of two diesel generators (DGs), a battery (BA), photo voltaic panels (PV), and a load, interconnected by a power grid with five admittances $Y_1 = 220.69 - 551.72i\ \Omega^{-1}$, $Y_2 = 172.28 - 470.13i\ \Omega^{-1}$, $Y_3 = 232.0 - 580.76i\ \Omega^{-1}$, $Y_4 = 86.2 - 215.52i\ \Omega^{-1}$ and $Y_5 = 43.10 - 107.76i\ \ \Omega^{-1}$. The base power of the MG is $S_{\text{grid}} = 100$ kVA.

We outline in this section how each component is modeled. Due to page number limitations, a more detailed description is beyond the scope of this work.

a) Power grid: The power grid consists of power lines, cables, transformers etc., which interconnect power system components. In principle, each power line and cable has its own dynamics. However, they have time constants which are orders of magnitude smaller than the time-scale of our NMPC scheme. For this reason, the dynamics of the interconnection elements are often neglected [12]. Consequently, the grid, i.e. the power flow, is typically described by the algebraic power flow equations:

$$P_i = \sum\nolimits_{j=1}^{N_\text{B}} V_i V_j \big(G_{ij} \cos \Delta\theta_{ij} + B_{ij} \sin \Delta\theta_{ij}\big), \quad \text{(3a)}$$

$$Q_i = \sum\nolimits_{j=1}^{N_\text{B}} V_i V_j \big(G_{ij} \sin \Delta\theta_{ij} - B_{ij} \cos \Delta\theta_{ij}\big), \quad \text{(3b)}$$

where N_B is the number of buses (nodes) in the power system, P_i and Q_i, are the injected active and reactive powers into the i-th bus (node) in the grid, V_i and θ_i are the magnitude and angle of the voltage phasor at the i-th bus, $\Delta\theta_{ij} = \theta_i - \theta_j$, and G_{ij} and B_{ij} are the elements of the conductance and susceptance matrix of the grid [12].

b) Diesel generators: Typical diesel generators consist of a synchronous generator with controllers and actuators, as shown in Fig. 2. We consider a model for the synchronous generator (SG_i) with 5 differential and 11 algebraic states, for details see [12]. The governor (GOV_i) controls the power generation P_i of the DG by controlling the diesel engine (DE_i). Its input is the generator frequency ω_i, as well as the reference power $P_{\text{ref},i}$. We use standard IEEE DEGOV1 model, shown in Fig. 3, to model DE_i and GOV_i of each DG. The GOV model consists of 8 differential and 2 algebraic states, whereby 3 of the differential states are due to the 3rd order Padé approximation with $T_\text{d} = 0.01$ s.

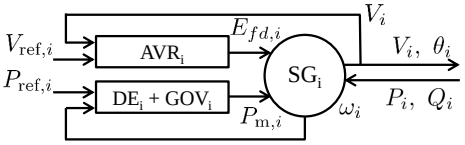

Fig. 2. Outline of a DG model. It consists of a synchronous generator (SG_i), automatic voltage regulator and exciter (AVR_i), and of a diesel engine (DE_i) and governor model (GOV_i).

The generator automatic voltage regulator (AVR_i) controls the terminal voltage of the generator via the field winding voltage $E_{\text{fd},i}$ from the exciter. In this work, we use the standard IEEE AC5A model shown in Fig. 4. The inputs to AVR_i are the reference voltage $V_{\text{ref},i}$, and the DG voltage V_i. The output of AVR_i is the field winding voltage $E_{\text{fd},i}$. The AVR model consists of 5 differential and one algebraic state. The two DGs in this MG have a nominal power of $S_{N_i} = 325$ kVA, $i = 1, 2$. In Fig. 2, $P_{\text{ref},i}$ and $V_{\text{ref},i}$ are used as control inputs for SC.

c) Battery: We model the battery as a constant DC voltage source connected to an inverter, which controls the voltage at its connection terminals. For the considered dynamics, modeling the high-frequency switching of power electronic elements in the inverters is often not necessary. Instead, the switching components in the inverters are approximated as ideal voltage sources with droop controllers for voltage amplitude and frequency, c.f. Fig. 5. The DC link capacitors of the inverters are not considered, as we

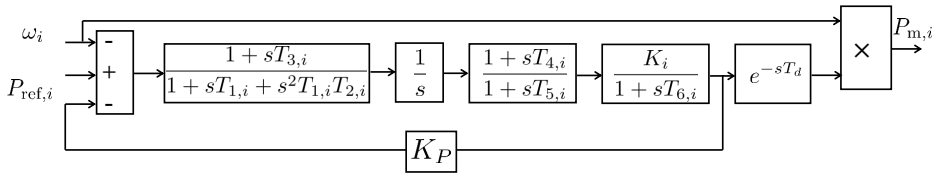

Fig. 3. The standard IEEE DEGOV1 model. The time delay block is approximated with the 3rd order Padé approximation.

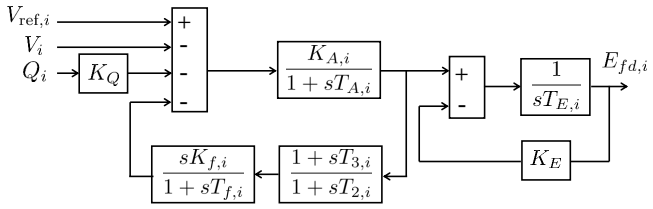

Fig. 4. The standard IEEE AC5A model used for AVR$_i$.

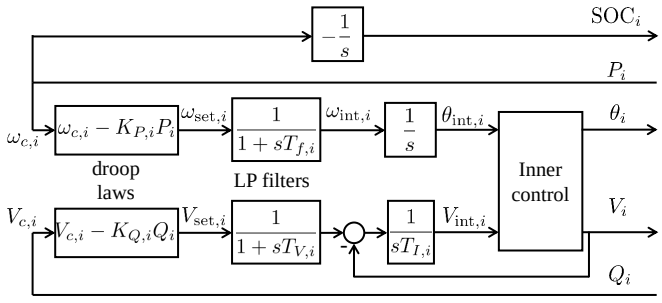

Fig. 5. Outline of a BA model. The state of charge (SOC) of the battery is an integral of the BA power P_i.

assume that the internal control of the inverters is fast enough to compensate for the changes on the DC side. Using such simplifications complies with measurements shown in [24].

The BA inverter controls the magnitude V_i and phase θ_i of the voltage on its terminals, whereas the active and reactive power infeed of the inverter result from the power flow. The reference frequency of the inverter $\omega_{\mathrm{set},i}$ is determined by a so-called droop equation

$$\omega_{\mathrm{set},i} = \omega_{c,i} - K_{P,i}P_i, \tag{4}$$

where $\omega_{c,i}$ is the frequency reference with zero load and is used as a control input for SC, P_i is the measured active power infeed of the i-th inverter, and $K_{P,i}$ is the frequency droop gain. The reference $\omega_{\mathrm{set},i}$ is filtered with a first-order low-pass filter with the time constant $T_{f,i}$ and integrated to obtain the internal voltage phase $\theta_{\mathrm{int},i}$. Analogously, the voltage reference $V_{\mathrm{set},i}$ is determined with a droop equation

$$V_{\mathrm{set},i} = V_{c,i} - K_{Q,i}Q_i, \tag{5}$$

where $V_{c,i}$ is the voltage reference with no reactive power generation, used as a control input for SC, $Q_{p,i}$ is the measured reactive power infeed of the i-th inverter, and $K_{Q,i}$ and is the frequency droop gain. The reference $V_{\mathrm{set},i}$ is filtered with a time constant $T_{\mathrm{v},i}$, and serves as the reference for the integral voltage controller. The output of the integral controller is the internal voltage $V_{\mathrm{int},i}$. The resulting $\theta_{\mathrm{int},i}$ and $V_{\mathrm{int},i}$ are used as references to the internal control loops which run at a much higher frequency. As the internal control loops are not modeled due to their fast dynamics, we assume $\omega_i = \omega_{\mathrm{int},i}$, $\theta_i = \theta_{\mathrm{int},i}$ and $V_i = V_{\mathrm{int},i}$. The BA is describe by in total 5 differential and 4 algebraic variables. The nominal power of the BA is $S_{N_3} = 150$ kVA and the capacity is 40 kWh.

d) PV and load: We model the active and reactive power infeeds P_i and Q_i of PV and load as the time-varying parameters $p(t)$ in the DAE (1). They both have predictable behavior, known from historic measurements and various commercially available forecast tools. Combining the models of all components with the power flow equations leads to the DAE of index 1 (1), where the algebraic equations arise from the algebraic power flow equations (3), as well as from internal algebraic equations of the DGs and BA.

The resulting model consists of 37 differential and 42 algebraic states. The control input $u \in \mathbb{R}^6$ gathers the reference active power $P_{\mathrm{ref},i}$ and voltage $V_{\mathrm{ref},i}$ of the DGs, as well as the reference frequency $\omega_{c,i}$ and voltage $V_{c,i}$ of the BA inverter.

IV. Optimization Problem Formulation

Isolated MGs usually have a centralized control room where all measurements are available [23]. By using these measurements, and the model of the power grid, all other states can be estimated as well. Since we have a full model and the applied algorithms and their implementations are real-time feasible for this problem scale, we take a centralized NMPC approach.

A. Cost Function

In our NMPC-based strategy for MG operation we consider the four following objectives:

a) Voltage Control: The first goal of our control policy is to keep the voltage on the load bus of the MG, close to 1 per unit (p.u.), as deviations from the nominal voltage may cause harm to the hardware. We achieve this goal with a least squares cost term:

$$L_1(x, z, u) = q\|V_6 - 1\|_2^2, \tag{6}$$

with V_6 being the algebraic variable representing the voltage on the bus where the load is connected, see Figure 1. We choose the weighting factor $q = 10^3$.

b) Frequency Control: Primary control, represented by proportional controllers with gains K_P and K_Q in Figs. 3-5, leaves a constant steady-state offset after changes in load. The next goal which we want to achieve is to keep the frequencies of the DERs in the MG close to 1 p.u., even in the presence of prediction mismatches and large disturbances, such as sudden large increase in demand or dropping out of large loads. This is achieved with the following least squares cost term:

$$L_2(x, z, u) = \|\omega - 1\|^2_{Q_2}, \tag{7}$$

where $\omega = [\omega_1,\ \omega_2,\ \omega_3]^\top$ is the vector of frequencies of the two diesel generators (nodes 1 and 2 in Figure 1) and the inverter frequency (node 3 in Figure 1). The diagonal weighting matrix is chosen as $Q_2 = \texttt{diag}(10^4,\ 10^4,\ 10^4)$.

c) Economic Goals: Beside operational goals, we want to fulfill economic goals such as minimizing the fuel costs of the DGs. This is achieved with the linear cost term

$$L_3(x, z, u) = cP_1 + cP_2, \tag{8}$$

where P_1 and P_2 are the corresponding active powers of the DGs in p.u. and c is the fuel cost which we take to be $c = 0.1$. Note that, in this work we consider an MG in islanded mode, hence we do not have market driven economic considerations, which are usually treated on a different time-scale [1]. It is straightforward to include other energy costs which can be due to market participation or prices obtained from an economic dispatch problem. Alternatively, the economic decisions from the tertiary level could be incorporated in our NMPC scheme as tracking references for active and reactive powers.

d) Load Sharing: To achieve islanded operation of the MG, the active and reactive power demand must be shared between the units in the MG according to predefined rules. For this purpose, we require that the units should share the active and reactive power production proportionally to their nominal (maximally available) power. Equal load sharing increases the robustness of the system to large disturbances, since they can be distributed among all DERs.

In our problem formulation, we penalize the deviation between the active and reactive power of the controllable production units, which we express with the following cost term:

$$\begin{aligned} L_4(x, z, u) = \rho \max_{\substack{i,j=1,2\\ i<j}} \left| \frac{P_i}{S_{N_i}} - \frac{P_j}{S_{N_j}} \right| \\ + \rho \max_{\substack{i,j=1,2,3\\ i<j}} \left| \frac{Q_i}{S_{N_i}} - \frac{Q_j}{S_{N_j}} \right|, \end{aligned} \tag{9}$$

where $\rho = 100$ is a weighting factor. The active and reactive power of all DERs are rescaled to p.u. w.r.t. their nominal powers. Note that we demand equal load share for reactive power between all devices, and for the active power just between the DGs. Otherwise, requiring that the battery has the same production as the DGs in p.u. would be in conflict with the requirement (8), which will be lower if the DGs produces less and the battery more. This cost term is nondifferentiable, but we can reformulate it by introducing slack variables and inequality constraints, see e.g. [25].

To achieve all the goals listed above, the cost function in our OCP (2) is given as the sum of the cost terms stated in (6), (7), (8) and (9).

B. Constraints

MGs have also operation limits prescribed by grid codes and due to hardware limitations. First, we impose a constraint on the voltage on all nodes:

$$0.9 \text{ p.u.} \leq V_i \leq 1.1 \text{ p.u.}, \quad i = 1, \ldots, 6. \tag{10}$$

Furthermore, all frequencies in the grid are allowed to be in the range of:

$$0.95 \text{ p.u.} \leq \omega \leq 1.05 \text{ p.u.}. \tag{11}$$

The production of active and reactive power by the DGs and the BA are limited by their nominal power:

$$P_i^2 + Q_i^2 \leq S_{N_i}^2, \quad i = 1, 2, 3. \tag{12}$$

Furthermore, due to physical limitations of the DGs , we demand a minimal $\cos(\phi_{\text{min}}) = 0.7$, which is expressed with the inequality:

$$P_i \geq \tan(\arccos(\phi_{\text{min}}))Q_i, \quad i = 1, 2. \tag{13}$$

Finally, the state of charge of the BA in our grid has to be:

$$0.1 \text{ p.u.} \leq \text{SOC}_3 \leq 1 \text{ p.u.}. \tag{14}$$

Together with the cost function, and the discretized DAE model these constraints evaluated at the discretization grid yield an NLP of the form (2), which we solve at every sampling instant. To our knowledge, there are no other practically relevant constraints. Also, in practice, grid losses are usually negligible compared to fuel costs, so we do not consider them in our problem formulation.

V. Simulation Results

To discretize the dynamics we apply direct multiple shooting [20] with the Gauss-Legendre Implicit Runge-Kutta scheme of order six with a fixed step-size $h = 0.1$ s and two intermediate integration steps. A prediction horizon of $T = 2$ s is used and the trajectories are discretized using $N = 20$ multiple shooting intervals. The NMPC feedback-rate is $T_{\text{s}} = 100$ ms. For a MG of this size we can neglect the communication delay, however one could easily use feedback delay compensation withing the AS-RTI scheme, with adapting the predicted state.

The time-varying load profile at node 6 and production profile of the PV at node 4 are depicted in Fig. 6. All quantities are in p.u. scaled to S_{grid}. Thereby, the blue lines show the true profiles, whereas the red lines show predicted ones. We use a load profile which emulates realistic conditions in an MG, see Fig. 6 (left plot). First, from $t = 1$ s to $t = 6$ s, we apply a load ramp. This emulates the gradual, predictable, load increase during the day. Afterwards, we apply an unpredicted load step at $t = 12$ s, which emulates

a sudden dropout of a large load. This load step is not a part of the prediction. And before it happens, the NMPC works with a larger predicted value, namely the same as right before $t = 12$ s. However, after it occurs, the prediction of the load is adapted to the new load value, which is represented by the dotted line in Fig. 6 (left plot). Finally, at $t = 20$ s, a predicted load step occurs, which can emulate an announced connection of a large load to the system. At this time-scale the PV profile does not change much, however PV production predictions can be incorporated into the OCP as well, see Fig. 6 (right plot).

In the simulation we compare three different approaches: 1) AS-RTI based NMPC controller, 2) fully converged NMPC controller and 3) a centralized I-controller for SC. We use an efficient implementation of the AS-RTI with a Gauss-Newton Hessian approximation in `acados` through its MATLAB interface. In the AS-RTI, in the preparation phase one additional Gauss-Newton SQP iteration is performed. For more details see references in Section II-B and [14]. For the fully converged NMPC the OCP is solved with the interior-point solver IPOPT [26] at every sampling instant using its interface in `CasADi` [27] in MATLAB. For this variant, instead of direct multiple shooting, we use the fully simultaneous approach with the same integrator, but with a single intermediate step and we use the exact Hessian. This results in a larger, but sparser NLP which is favorable for interior-point solvers [28]. The integral gain of the I-controller is chosen to be $K_I = 0.125$, which emulates realistic state-of-the-art operation of SC [4]. Note that an I-controller cannot be trivially used for voltage and reactive power (V-Q) control, because the primary V-Q control uses local voltage measurement V_i. Due to the power flow, cross coupling between the primary controllers arises for which more complex control laws, such as NMPC, become necessary.

The simulation results for the above approaches are depicted in Fig. 7. One can see on the top plot that the frequencies ω closely follow 1. In contrast to the I-controller, the NMPC controller eliminates the steady-state offset during the load ramp. Furthermore, after the unpredicted load drop at $t = 12$ s, the frequency ω returns to the nominal value much faster when NMPC is used. Note that the overshoot remains the same because the load step is not in the prediction, and NMPC can react only after the time T_s has passed. Furthermore, when the load step is known to the NMPC controller (at $t = 20$ s) the overshot is significantly smaller compared to the I-controller. Moreover, the frequencies are quickly at 1 p.u. again and the I-controller needs several seconds to achieve this. With NMPC the voltage at node 6 is successfully kept at 1 p.u., and all other voltages are kept in the prescribed bounds (10), which is not possible with conventional I-controllers, see second plot in Fig. 7. In the third and bottom plot one can see that equal load share is successfully achieved with the NMPC controller. Thereby, P_1 and P_2 have the same value and the battery is producing with its maximal power, which reduces the fuel costs as required by the cost terms (8) and (9).

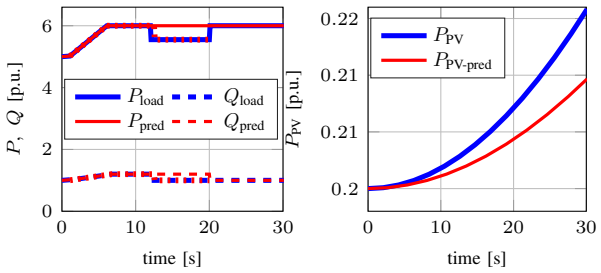

Fig. 6. Load profile (left) and PV production profile (right) in p.u..

TABLE I
CPU TIMES OF DIFFERENT NMPC SCHEMES IN MILLISECONDS.

Algorithm	**Preparation Phase**			**Feedback Phase**		
	max	min	mean	max	min	mean
IPOPT	2851.30	870.53	1354.30	0[1]	0	0
AS-RTI	78.14	62.19	64.78	6.77	3.11	3.94

The CPU times of AS-RTI and fully converged NMPC schemes are given Table V. All simulation are run on HP Z-book equipped with an Intel i7-6820HQ CPU with 2.70 GHz and 16 GB RAM. In contrast to the fully converged solution, the efficient implementation of AS-RTI for DAEs in `acados` is real-time feasible for the chosen sampling rate with an average feedback delay of no more than 4 ms. Compared to the centralized I-controller with the proposed real-time NMPC approach several important improvements can be achieved: 1) we can reduced the settling time by factor of approximately 2 when there is an unknown step disturbance, 2) eliminate the steady-state offset when there is a load ramp, 3) we can reduce the overshoot when there is a known load step, 4) equal steady-state active and reactive load sharing is achieved, 5) fuel cost of the DGs are reduced.

VI. Conclusion and Outlook

In this paper we presented a real-time feasible NMPC scheme for optimal operation of MGs. The MG was modeled with a large and complex DAE of index 1. For the NMPC algorithm we used the recently introduced AS-RTI scheme and its implementation in the software package `acados`. We demonstrate in this work that, with the presented approach we are able to successfully control the frequency, voltage and fulfill load sharing and economic goals at the same time. Recent developments both in algorithms and software made it possible to control even a complex MG with fast dynamics in real-time in a centralized way. Our proposed scheme outperforms a state-of-the-art I-controller for SC and shows minor difference in performance compared to a fully converged NMPC controller.

One of the next natural goals is to explore the capability of this control approach for even larger grids with more devices. Next, it would be interesting to investigate the operation of

[1] Since the fully converged approach is not real-time feasible, in the simulation we act like the solution is immediately available and no feedback delay is present, i.e. we have instantaneous NMPC without delay. Otherwise, the controller performance is severely harmed and does not serve as a good reference for comparison. The CPU times of this approach are reported in the preparation phase columns.

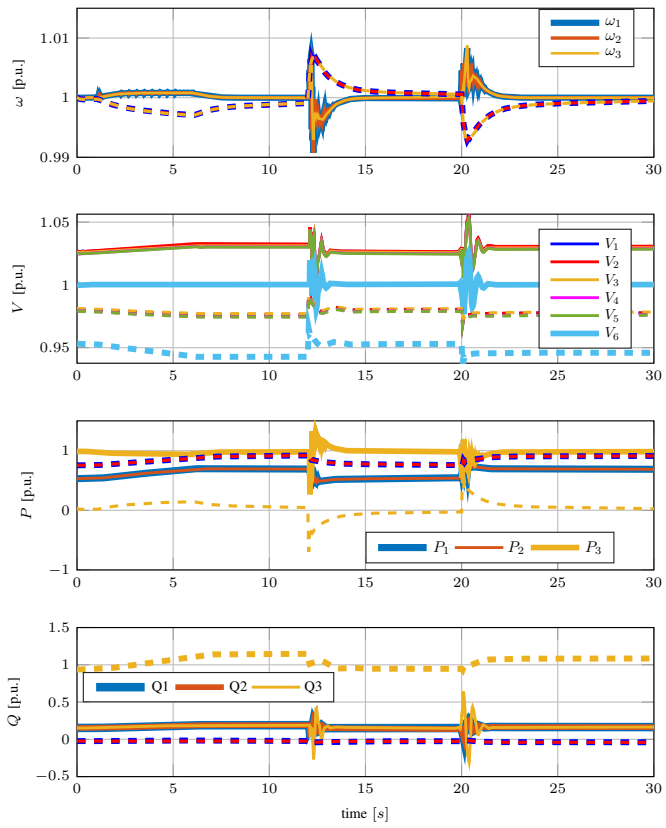

Fig. 7. Frequencies, voltages, active and reactive power for the considered MG. The solid lines are for the NMPC controller and the dashed for the I-controller. The difference between fully converged NMPC and AS-RTI is minor, so we plot just one of them to keep the plots clear. The top plot depicts the frequencies ω of the DERs. The second plot show the voltage at all nodes in the MGs. The third and bottom plot show the active and reactive powers of the DERs, respectively.

MG with NMPC in a grid-connected scenario, possibly in a hierarchical fashion to consider also market-driven energy costs.

References

[1] A. Parisio, E. Rikos, and L. Glielmo, "A model predictive control approach to microgrid operation optimization," *IEEE Transactions on Control Systems Technology*, vol. 22, no. 5, pp. 1813–1827, 2014.

[2] G. Lou, W. Gu, Y. Xu, M. Cheng, and W. Liu, "Distributed mpc-based secondary voltage control scheme for autonomous droop-controlled microgrids," *IEEE transactions on sustainable energy*, vol. 8, no. 2, pp. 792–804, 2016.

[3] P. Braun, T. Faulwasser, L. Grüne, C. M. Kellett, S. R. Weller, and K. Worthmann, "Hierarchical distributed admm for predictive control with applications in power networks," *IFAC Journal of Systems and Control*, vol. 3, pp. 10–22, 2018.

[4] J. Simpson-Porco, Q. Shafiee, F. Dörfler, J. Vasquez, J. Guerrero, and F. Bullo, "Secondary frequency and voltage control of islanded microgrids via distributed averaging," *IEEE Transactions on Industrial Electronics*, vol. 62, no. 11, pp. 7025–7038, 2015.

[5] Y. Han, H. Li, P. Shen, E. A. A. Coelho, and J. M. Guerrero, "Review of active and reactive power sharing strategies in hierarchical controlled microgrids," *IEEE Transactions on Power Electronics*, vol. 32, no. 3, pp. 2427–2451, 2016.

[6] F. Delfino, R. Minciardi, F. Pampararo, and M. Robba, "A multilevel approach for the optimal control of distributed energy resources and storage," *IEEE Transactions on Smart Grid*, vol. 5, no. 4, pp. 2155–2162, 2014.

[7] C. Ahumada, R. Cárdenas, D. Saez, and J. M. Guerrero, "Secondary control strategies for frequency restoration in islanded microgrids with consideration of communication delays," *IEEE Transactions on Smart Grid*, vol. 7, no. 3, pp. 1430–1441, 2015.

[8] A. Parisio and L. Glielmo, "Energy efficient microgrid management using model predictive control," in *2011 50th IEEE Conference on Decision and Control and European Control Conference*, pp. 5449–5454, IEEE, 2011.

[9] A. Venkat, I. Hiskens, J. Rawlings, and S. Wright, "Distributed MPC strategies with application to power system automatic generation control," *IEEE Trans. Control Syst. Technol.*, vol. 16, no. 6, pp. 1192–126, 2008.

[10] A. M. Ersdal, L. Imsland, and K. Uhlen, "Model predictive load-frequency control," *IEEE Transactions on Power Systems*, vol. 31, no. 1, pp. 777–785, 2015.

[11] P. Malysz, S. Sirouspour, and A. Emadi, "An optimal energy storage control strategy for grid-connected microgrids," *IEEE Transactions on Smart Grid*, vol. 5, no. 4, pp. 1785–1796, 2014.

[12] P. Kundur, *Power System Stability and Control*. McGraw-Hill, 1993.

[13] R. Scholz, A. Nurkanović, A. Mešanović, J. Gutekunst, A. Potscka, H. G. Bock, and E. Kostina, "Model-based Optimal Feedback Control for Microgrids with Multi-Level Iterations," *Submitted to Operations Reserach 2019*, 2019.

[14] A. Nurkanović, A. Zanelli, S. Albrecht, and M. Diehl, "The Advanced Step Real Time Iteration for NMPC," in *2019 IEEE 58th Conference on Decision and Control (CDC)*, pp. 5298–5305, Dec 2019.

[15] A. Nurkanović, A. Zanelli, G. Frison, S. Albrecht, and M. Diehl, "Contraction Properties of the Advanced Step Real-Time Iteration," in *Proceedings of the IFAC World Congress*, vol. 51, 2020.

[16] R. Verschueren, G. Frison, D. Kouzoupis, N. van Duijkeren, A. Zanelli, B. Novoselnik, J. Frey, T. Albin, R. Quirynen, and M. Diehl, "acados: a modular open-source framework for fast embedded optimal control," *arXiv preprint*, 2019.

[17] A. Nurkanović, S. Albrecht, and M. Diehl, "Multi Level Iterations for Economic Nonlinear Model Predictive Control," in - (T. Faulwasser, M. A. Müller, and K. Worthmann, eds.), Springer, 2019.

[18] J. Frey, R. Quirynen, D. Kouzoupis, G. Frison, J. Geisler, A. Schild, and M. Diehl, "Detecting and exploiting Generalized Nonlinear Static Feedback structures in DAE systems for MPC," in *Proceedings of the European Control Conference (ECC)*, 2019.

[19] G. Frison and M. Diehl, "HPIPM: a high-performance quadratic programming framework for model predictive control," *arXiv preprint arXiv:2003.02547*, 2020.

[20] H. G. Bock and K. J. Plitt, "A multiple shooting algorithm for direct solution of optimal control problems," in *Proceedings of the IFAC World Congress*, pp. 242–247, Pergamon Press, 1984.

[21] M. Diehl, *Real-Time Optimization for Large Scale Nonlinear Processes*. PhD thesis, University of Heidelberg, 2001.

[22] G. Frison, D. Kouzoupis, T. Sartor, A. Zanelli, and M. Diehl, "BLASFEO: Basic linear algebra subroutines for embedded optimization," *ACM Transactions on Mathematical Software (TOMS)*, vol. 44, no. 4, pp. 42:1–42:30, 2018.

[23] Siemens, "Siemens provides sustainable energy for galapagos island." `https://www.siemens.com/press/en/pressrelease/?press=/en/pressrelease/2018/energymanagement/pr2018120097emen.htm&content[]=EM`.

[24] A. Mešanović, U. Münz, A. Szabo, M. Mangold, J. Bamberger, M. Metzger, C. Heyde, R. Krebs, and R. Findeisen, "Guaranteed $\mathcal{H}_\infty$ controller parameter tuning for power systems: Method and experimental evaluation," *Control Engineering Practice, submitted*, 2019.

[25] J. Nocedal and S. J. Wright, *Numerical Optimization*. Springer Series in Operations Research and Financial Engineering, Springer, 2 ed., 2006.

[26] A. Wächter and L. T. Biegler, "On the implementation of an interior-point filter line-search algorithm for large-scale nonlinear programming," *Mathematical Programming*, vol. 106, no. 1, pp. 25–57, 2006.

[27] J. A. E. Andersson, J. Gillis, G. Horn, J. B. Rawlings, and M. Diehl, "CasADi: a software framework for nonlinear optimization and optimal control," *Mathematical Programming Computation*, 2018.

[28] J. B. Rawlings, D. Q. Mayne, and M. M. Diehl, *Model Predictive Control: Theory, Computation, and Design*. Nob Hill, 2nd edition ed., 2017.